Food Chemistry 410 (2023) 135395

Contents lists available at ScienceDirect

Food Chemistry

journal homepage: www.elsevier.com/locate/foodchem

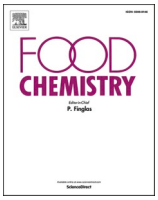

Effect of ferulic acid derivative concentration on the release kinetics, antioxidant capacity, and thermal behaviour of different polymeric films

Muhammad Rehan Khan [a,b], Sami Fadlallah [b,*], Antoine Gallos [b], Amandine L. Flourat [b], Elena Torrieri [a], Florent Allais [b,*]

[a] Department of Agricultural Science, University of Naples Federico II, Via Università 133, 80055 Portici, Italy
[b] URD Agro-Biotechnologies Industrielles (ABI), CEBB, AgroParisTech, 3 Rue des Rouges-Terres, 51110 Pomacle, France

ARTICLE INFO

Keywords:
Release kinetics
Mathematical modelling
Ferulic acid derivative
PHAs and PLA
Antioxidant activity
Thermal behavior

ABSTRACT

Ferulic acid displays poor thermal resistance during extrusion and compression moulding, slow 2,2-diphenyl-1-picrylhydrazyl (DPPH) reaction kinetics, and undetected release from polylactide (PLA) and polyhydroxyalkanoates (PHA)-based films into polar media. Thus, in this study, a ferulic acid derivative Bis-*O*-dihydroferuloyl-1,4-butanediol (BDF) was used as an active additive (up to 40 w%) in PLA, poly(3-hydroxybutyrate) (PHB), and poly(3-hydroxybutyrate-*co*-3-hydroxyvalerate) (PHBV) matrices to produce blends by extrusion. These blends were then used to prepare films by solvent casting. The BDF displayed good stability with 86–93% retention. The release kinetics in Food Simulant A revealed higher BDF release amounts (1.16–3.2%) for PHA-based films as compared to PLA. The BDF displayed faster DPPH reaction kinetics as compared to ferulic acid. The PHA-based films containing BDF displayed > 80% of DPPH inhibition. The growth of crystals inside polymer matrix had a nucleation effect which reduced the glass transition temperature of the films.

1. Introduction

Petroleum-based plastics have surpassed most man-made materials, leading to a global environmental crisis. For example, plastic production accounts for ~40% of the total production of the packaging industry, encouraging the food packaging industry to seek more sustainable materials as alternatives for ensuring food quality and safety (Foschi and Bonoli, 2019). Biodegradable bioplastics represent an alternative way to develop sustainable food packaging (Foschi and Bonoli, 2019).

Polylactide (PLA) has recently gained tremendous attention in the food packaging industry due to its safety, compostability under controlled conditions, sustainability, and biocompatibility. PLA is a renewable linear thermoplastic polyester that is produced by ring-opening polymerization of lactide at the industrial scale (Rojas et al., 2021). However, low thermal resistance and inherent brittleness restrict its application in food packaging (Ordoñez, Atarés, and Chiralt, 2022a). Other thermoplastic polyesters include polyhydroxyalkanoates (PHAs), such as poly(3-hydroxybutyrate) (PHB), which are intracellular energy and carbon storage compounds found in some soil bacteria and possess similar melting temperatures as petro-chemical based plastics i.e., polypropylene (Carboué et al., 2022). However, due to the low glass transition temperature (1–10 °C), PHB is highly brittle in nature (Fiorese et al., 2009). Nonetheless, the copolymer poly(3-hydroxybutyrate-*co*-3-hydroxyvalerate) (PHBV) can serve as an alternative to PHB because of its higher biocompatibility, lower melting temperature, and comparatively lower crystallinity. However, low thermal stability and difficult processability limit its application in the food industry (Ibrahim, Alsafadi, Alamry, and Husssein, 2021). In this sense, their functional properties can be enhanced by incorporating active compounds as additives into the polymer matrix which not only add value to the material, and increase its competitiveness in the packaging market, but also enhance the ability of the packaging for food preservation.

An interesting area in food packaging is the development of active releasing systems. Active releasing packaging is a novel interaction between the packaging and the food product by releasing active compounds from the polymer matrix into the food surface to extend its shelf life (Tawakkal, Cran, Miltz, and Bigger, 2014). One of the biggest challenges in developing an active releasing system is to modulate its ability to release bioactive compounds in an optimum concentration to restrict the nutritional losses owing to oxidation reactions. For instance,

* Corresponding authors.
E-mail addresses: sami.fadlallah@agroparistech.fr (S. Fadlallah), florent.allais@agroparistech.fr (F. Allais).

https://doi.org/10.1016/j.foodchem.2023.135395
Received 5 September 2022; Received in revised form 13 December 2022; Accepted 2 January 2023
Available online 3 January 2023

ferulic acid is a *p*-hydroxycinnamic acid present in plants and that has a variety of biological activities i.e., antimicrobial, antioxidant, and anticancer, and is commonly used as an additive for the manufacturing of PLA and PHA-based active releasing films by using extrusion, compression moulding, and melt-blending (Hernández-García, Vargas, and Chiralt, 2022). Several studies have reported improved mechanical, barrier, optical, thermal, and biodegradable properties due to the addition of ferulic acid into PLA and PHA-based systems (Ordoñez et al., 2022a; Ordoñez, Atarés, and Chiralt, 2022b). However, a loss of ~30% of the ferulic acid mass has been reported during the preparation of the active PLA/PHA-based releasing systems due to the presence of one phenolic hydroxyl group (Ordoñez et al., 2022a). Another drawback of incorporating ferulic acid in PLA blends is their non-detectable release into the polar food simulants (i.e., Food Simulant A; which are used to mimic fruits and vegetables) due to the nature, structure, and interactions between the polymer and the bioactive, on the other hand, absence of polymer relaxation could also promote non-detectable ferulic acid release behaviour (Ordoñez et al., 2022a). Furthermore, the slow antioxidant reaction kinetics of ferulic acid, due to its monophenolic structure, can hinder its application as a package to restrict oxidation kinetics (Goujot, Cuvelier, Soto, and Courtois, 2019).

Ferulic acid can be modified to produce ferulic acid derivatives such as Bis-*O*-dihydroferuloyl-1,4-butanediol (BDF) which can have a positive impact on the mechanical, thermal, and biodegradation properties of PHA and PLA-based materials, and maybe on the release kinetics and antioxidant capacity (Carboué et al., 2022; Pion, Reano, Ducrot, and Allais, 2013; Raghuwanshi et al., 2022). For instance, the addition of 40 w% BDF content into PLA and PHA blends improved the elongation at break 82 and 4 times more, respectively, as compared to the neat samples (Gallos et al., 2021; Longé et al., 2022). Similarly, the addition of BDF (5–40 w%) into PHB blends resulted in faster biodegradation (1.3–3 times) of the PHB/BDF blends by *Actinomucor elegans* in the soil as compared to neat PHB samples; since fungi can degrade and metabolize *p*-hydroxycinnamic acids i.e., ferulic acid which is a structural compound in the lignocellulosic matrix (Carboué et al., 2022). BDF can provide detectable release from PLA/PHA matrices into polar media by causing polymer relaxation due to its plasticizing properties or by affecting the polymer's glass transition temperature. On the other hand, the presence of bi-phenolic OH-groups in BDF can improve the thermal resistance and antioxidant capacity of both additive and the polymerc system (Longé et al., 2022). For instance, BDF displayed higher thermal resistance with a mass loss of 10% at 285–298 °C as opposed to 205–210 °C of ferulic acid. Ferulic acid derivatives i.e., BDF are also thermally stable during extrusion and injection processes (175–185 °C) (Kasmi, Gallos, Beaugrand, Paës, and Allais, 2019). Similarly, the antioxidant reaction kinetics of BDF can be much faster than ferulic acid due to its modified structure since ferulic acid requires the formation of biferulic acid before reducing 2,2-diphenyl-1-picrylhydrazyl radical (DPPH·) (Aragón-Gutiérrez et al., 2020; Goujot et al., 2019).

The release kinetics and the partition coefficient of the active compound from the polymer matrix into the complex food systems are greatly influenced by the additive-polymer interactions, potential relaxation of the polymer upon contact with the food simulant, and the chemical affinity of the compounds toward polymer/food simulant. These factors define the concentration of the bioactive in the simulant as a function of time. Contrarily, the release of the active compound is influenced by the polymer nature, the environmental conditions, and the molecular characteristics of the additive; for instance, the release rate is faster when governed by swelling and slower when governed by diffusion in the polymer matrix (Ordoñez et al., 2022a; Requena, Vargas, and Chiralt, 2017). Therefore, the development of active PLA, PHB, and PHBV films containing BDF requires the verification of the influence of bioactive on the functional attributes of the polymer as well as on the efficient release to exert the antioxidant effect on a particular system. Since there was no study on the influence of BDF concentration on different polymeric films, the objective of this study was to develop PLA, PHB, and PHBV films with BDF at different concentrations (0, 10, 20, and 40 w%) for packaging applications. The influence of BDF incorporation on the release kinetics was investigated in the polar medium. Furthermore, the chemical structure was evaluated to understand the dynamics of chemical fingerprinting before and after release kinetics. Antioxidant capacity was analysed by using DPPH reaction kinetics as a benchmark. Finally, thermal properties were also investigated.

2. Materials and methods

2.1. Materials

PHB and PHBV powder were acquired from BIOMER (Schwalbach am Taunus, Germany). The PLA was purchased from NatureWorks (Ingeo™ 4043D, Minnesota, USA). The BDF was synthesised from ferulic acid with a protocol described elsewhere (Pion et al., 2013). 2,2-diphenyl-1-picrylhydrazyl (DPPH) was acquired from Fischer Scientific (Illkirch, France). Ethanol and chloroform were purchased from VWR Chemicals BDH (Radnor, PA, USA). All other reagents used were of analytical grade.

2.2. Methods

2.2.1. Preparation of polymer/BDF specimens by extrusion

Extrusion of the polymer/BDF blends was performed by the method given by Longé et al. (2022) by using a compounding twin screw extruder HAAKE MiniLab II (Thermo Fischer Scientific, Waltham, MA, USA). Briefly, blends with polymers (PHB or PHBV) and BDF weight ratios (100:0, 90:10, 80:20, and 60:40) were extruded at 170 °C at 60 rpm by setting the screws in co-rotation, while for PLA samples extruded at 180 °C at 50 rpm were used (Gallos et al., 2021). The moulding of the samples was carried out by the HAAKE MiniLab Pro Piston Injection Moulding System. A DMA test bar mould was used with dimensions of 60 mm × 10 mm × 1 mm. During the injection, 45 °C temperature was used to maintain the mould.

2.2.2. Film preparation

The solvent casting method given by Carboué et al. (2022) was used with slight modifications to prepare the different film samples (PHBV/BDF, PHB/BDF, and PLA/BDF). Briefly, the polymer/BDF blends (533 mg) obtained previously were dissolved in chloroform (26.6 mL) and the solution was then poured into stainless steel rectangular moulds (Dimensions: 7.5 cm × 2.5 cm). To obtain uniform film samples, the solvent was evaporated at room temperature under a fume hood. The steel moulds were covered with cardboard to prevent the effect of the hood from destabilizing the films.

2.2.3. Retention of bioactive in the films after processing

The remaining content of BDF in the films was determined by a method given by Woranuch, Yaksan, and Akashi (2015) with modifications. In brief, BDF in each film sample (1 cm^2) was extracted with 10 mL of chloroform at 40 °C for 48 h. The extracted solution was then analysed by using a UV–vis spectrophotometer (Cary 60, Agilent Technologies, CA, USA) at a wavelength of 280 nm. The remaining content was calculated by using a standard calibration curve ($y = 0.0013\times$, $R^2 = 0.9904$).

2.2.4. Release kinetics of BDF

The specific migration of BDF from different polymeric films was evaluated by using Food Simulant A (10% ethanol) according to European Commission (EC) regulation 10/2011 (since Food Simulant A can be used to mimic fruits and vegetables) by following the protocol previously established by Khan, Volpe, Salucci, Sadiq, and Torrieri (2022) with slight modifications. The film samples (4 cm^2) were completely immersed (double-sided) into the food simulant at room temperature. The UV–vis Spectrophotometer (Cary 60, Agilent Technologies, CA,

USA) was used to determine the concentration of BDF released from the films into the simulant at 280 nm. The samples were taken out at regular intervals of time (0, 24, 48, 144, 216, and 240 h) to quantify the concentration of the bioactive by using a standard calibration curve for BDF (150–600 μg/mL). The results were expressed as μg/mL of the simulant.

2.2.5. Mathematical modelling

The mathematical models are useful in describing the release behaviour of a bioactive from the polymeric chains of a film into the food simulant by using Fick's Second Law. The migration process was elucidated by the diffusion coefficient (D) and partition coefficient (K) of the migrant molecules. The following assumptions were considered by using a relationship derived from Fick's Second Law for a plane sheet to determine the diffusion coefficient of BDF from the experimental data (Niaz and Imran, 2021): a) initial concentration of BDF was homogenous throughout the film, b) the material was homogenous and isotropic, c) initial concentration of the BDF was zero in the food simulant solution, d) influence of swelling upon the kinetics of mass transfer was supposed negligible, e) the amount of BDF diffused from the film into simulant was increased in the concentration of the migrant from zero ($C_{f,0}$) to equilibrium ($C_{f,\infty}$), and f) the effective diffusivity should be considered constant. This model considered a limited volume of a plane sheet (film) in a limited volume of solution (food simulant), and if we consider that diffusion occurred from both sides of the film; Fick's Law can be solved numerically rather than analytically by using finite differences methodology (in which we solve the non-linear terms of the partial differential equation (PDE), where the unknown variable is the migrant concentration at each nodal point of the system). The Fick's Model, boundary conditions, and differential equations are as follows:

$$\frac{\partial C(x,t)}{\partial t} = D\left[\frac{\partial^2 C(x,t)}{\partial x^2}\right] \tag{1}$$

$$\begin{cases} \left.\dfrac{dc_i(t)}{d_t}\right|_{i=0} = 0 \\ \left.\dfrac{dc_i(t)}{d_t}\right|_{i=n} = 0 \end{cases} \tag{2}$$

Whereas C is the ratio of the concentration of BDF at time t and its concentration after infinity. Furthermore, to simplify the solution of PDE of the Fick's Law, the method of lines was used with respect to the spatial variable on the second derivative. This approximation transforms the PDE into an ordinary differential equation (ODE):

$$\frac{dC_i t}{dt} = D\frac{(C_{i-1}(t) - 2C_i(t) + C_{i+1}(t))}{x^2} \tag{3}$$

x is the distance from the interface obtained by dividing the thickness of the film (e) to the total number of layers (η).

$$C = \frac{M_{f,t}}{M_{f,\infty}} \tag{4}$$

$$x = \frac{e}{\eta} \tag{5}$$

For ensuring the validation of mathematical models and the goodness of fit of the predicted data with experimental by minimizing the sum of square of the differences between measured and predicted values, root mean square error (RMSE) was calculated by using MATLAB (version R2022a, MathWorks, USA).

$$RMSE = \sqrt{\frac{\sum_{i=1}^{N}(\hat{y}_i - y_i)^2}{N}} \tag{6}$$

where $\hat{y}_i$ and y_i are the residual values of observed and predicted values respectively while N is the number of the experimental point (Khan et al., 2022).

Partition coefficient can be described as the ratio of the BDF in the food simulant ($C_{s,\infty}$) to the BDF in the polymer matrix ($C_{f,\infty}$) once plateau is reached:

$$K = \frac{c_{s,\infty}}{c_{f,\infty}} \tag{7}$$

2.2.6. Fourier-transform infrared (FT-IR) spectroscopy

The chemical fingerprinting of all the film samples before and after release kinetics was evaluated through Fourier-transform infrared (FT-IR) spectroscopy by using FT-IR Spectrometer (Cary 630, Agilent Technologies, CA, USA). The spectra were recorded in the middle infrared (4000–650 cm^{-1}) range using absorbance mode with a resolution of 4 cm^{-1}. For each spectrum, 8 scans were co-added.

2.2.7. Antioxidant activity

The DPPH radical scavenging method is a globally followed and accepted method for measuring the antioxidant capacity of the polymeric materials. The methodology is based on the reduction of a stable DPPH· radical by means of an antiradical compound as a function of time (Khan, Di Giuseppe, Torrieri, and Sadiq, 2021). However, there are certain assumptions that should be kept in mind while measuring the antioxidant capacity of a compound: a) the antioxidant capacity of an antioxidant depends upon its chemical structure, b) the reaction can be fast (<30 min), slow (>60 min), or moderate (30–60 min) depending upon the ability of the antioxidant to reduce the DPPH· radical, c) contact time of the antioxidant with DPPH radical should be respected as the antioxidant molecules will not be able to express all the antioxidant activity and will remain unused, thus we will have incorrect antioxidant capacity, d) choice of solvent affect the kinetics parameters i.e., the balance between HAT and SET mechanism, and e) ferulic acid is a slow antioxidant due to its monophenolic structure, while BDF can display better reaction rate due to its diphenolic structure (Goujot et al., 2019).

Considering the above facts, the antioxidant activity of the film samples was measured by method given Priyadarshi, Kim, and Rhim (2021) with modifications. Briefly, an ethanolic solution of DPPH was prepared by dissolving 2.5 mg of DPPH in 100 mL of ethanol. 1 cm^2 of each film sample was added into 10 mL of ethanol, incubated for two different contact times (30 min and 90 min) in the dark at room temperature and the absorbance was measured at 517 nm. The same test without a film sample was used as a control. The antioxidant capacity of the film samples was calculated as percentage DPPH inhibition and was as follows:

$$Antioxidant\ activity(\%) = \frac{AC - AS}{AC} \times 100 \tag{8}$$

Where AC (0.6551) is the absorbance of the control and AS is the absorbance of the sample.

2.2.8. Thermal analysis

Thermogravimetric analysis (TGA)

TGA was performed by using TGA Q500 (TA Instruments, NC, USA) under nitrogen flow. Approximately, 3–7 mg of the film samples were equilibrated at 50 °C for 30 min. Then the samples were heated from 50 °C to 500 °C at 10 °C/min. The results were presented as graphs representing weight loss of the film samples as opposed to temperature.

Differential scanning calorimetry (DSC)

DSC was performed by using a DSC Q20 (TA Instruments, NC, USA). ~4–10 mg film samples were placed in a sealed pan flushed with pure nitrogen gas. The first heating scan was performed from −80 °C to 200 °C at a heating rate of 10 °C/min and was used to determine the melting temperature (T_m). This was followed by a cooling run to −80 °C with a cooling ramp of 200 °C/min. The glass transition temperature (T_g) was obtained during the second heating scan from −80 °C to 200 °C at 10 °C/min rate (Carboué et al., 2022).

2.2.9. Statistical analysis

One-way analysis of variance (ANOVA) and independent *t*-test were performed to estimate the significant difference ($p < 0.05$) among mean observations (SPSS, version 27.0, Chicago, IL, USA). All the experiments were performed in triplicates.

3. Results and discussion

3.1. Quantification of BDF in the films

The quantification of the final amount of BDF remaining in the active films is important since, at high temperatures during extrusion process, significant losses of bioactive compounds can occur due to thermal degradation or chemical reaction i.e., cross-linking or trans-esterification. It was observed that similar amount of BDF was recovered from each film sample (PHB and PHBV) indicating good homogeneity of BDF at macromolecular level. However, the total amount of BDF recovered from films with 10 w%, 20 w% and 40 w% BDF content was only 89.85 ± 1.61%, 91.40 ± 0.32%, and 93.42 ± 2.11%, respectively of the initial amount introduced during the extrusion process, and irrespective of the polymeric material used (PHB and PHBV). However, for PLA, the total amount of BDF recovered was 86.50 ± 3.13%, 89.96 ± 0.75%, and 91.70 ± 0.38%. Thus, the thermal process induced ~6.5–13.5% of BDF mass loss, that could be attributed to both thermal degradation, chemical interactions, and oxidation reactions since no volatile compounds are generated at such high temperatures (i.e., 170–180 °C). It can be observed that the amount of remaining BDF increased with increasing concentration of BDF in the films, this phenomenon has already been reported for ferulic acid-based EVOH (ethylene vinyl alcohol) films which underwent melt extrusion at 180 °C (Aragón-Gutiérrez et al., 2020). According to Ramos, Jiménez, Peltzer and Garrigós (2014) residence time of mixture in the extruder, additive concentration, degree of volatility of the additive, and extrusion temperature are the main factors affecting the final concentration of the additive in the blend. A loss of 30–40% have been reported for the polymer materials containing ferulic acid in literature after melt/blown extrusion, however we only observed ~13.5% BDF loss because BDF contains two phenolic hydroxyl groups as opposed to ferulic acid which contains only one, thus show more thermal stability than ferulic acid. The TGA results also validated this fact since ferulic acid displayed a mass loss of 10% at ~210 °C as opposed to BDF which displayed similar mass loss at ~290 °C (Aragón-Gutiérrez et al., 2020; Santos et al., 2012). These results were in accordance with results observed for thermo-processed PLA films containing ferulic acid (Ordoñez et al., 2022a).

3.2. Release kinetics of BDF

Release kinetics of a bioactive compound is important to study since not only it has a role in controlling the quality of the food product but also in meeting the migration limits set by regulatory authorities. To mimic the fruits and vegetables, 10% ethanol was selected as a Food simulant (Food simulant A) to elucidate the release of BDF from the film into the simulant. Fig. 1 displays the release of different BDF concentrations from different polymeric materials (i.e., PHBV, PHB, and PLA). There was a significant difference ($p < 0.05$) in the amount of BDF released with increasing concentration of BDF in the matrix. A significant increase in the release of BDF was observed from all the film samples in the initial 48 h, followed by equilibrium. The highest concentration of BDF released was (465 μg/mL, 759 μg/mL, and 101 μg/mL) observed for film samples containing 20 w% BDF (PHBV, PHB, and PLA, respectively) irrespective of the polymer type used. The polymer and bioactive nature, structure, and affinity toward food simulant, are some of the parameters that influence the release of bioactive from the film into the simulant (Khan et al., 2022). In accordance with the above fact, the films with low BDF concentration (i.e., 10–20 w%) displayed a higher release percentage ($p < 0.05$) as compared to films with the

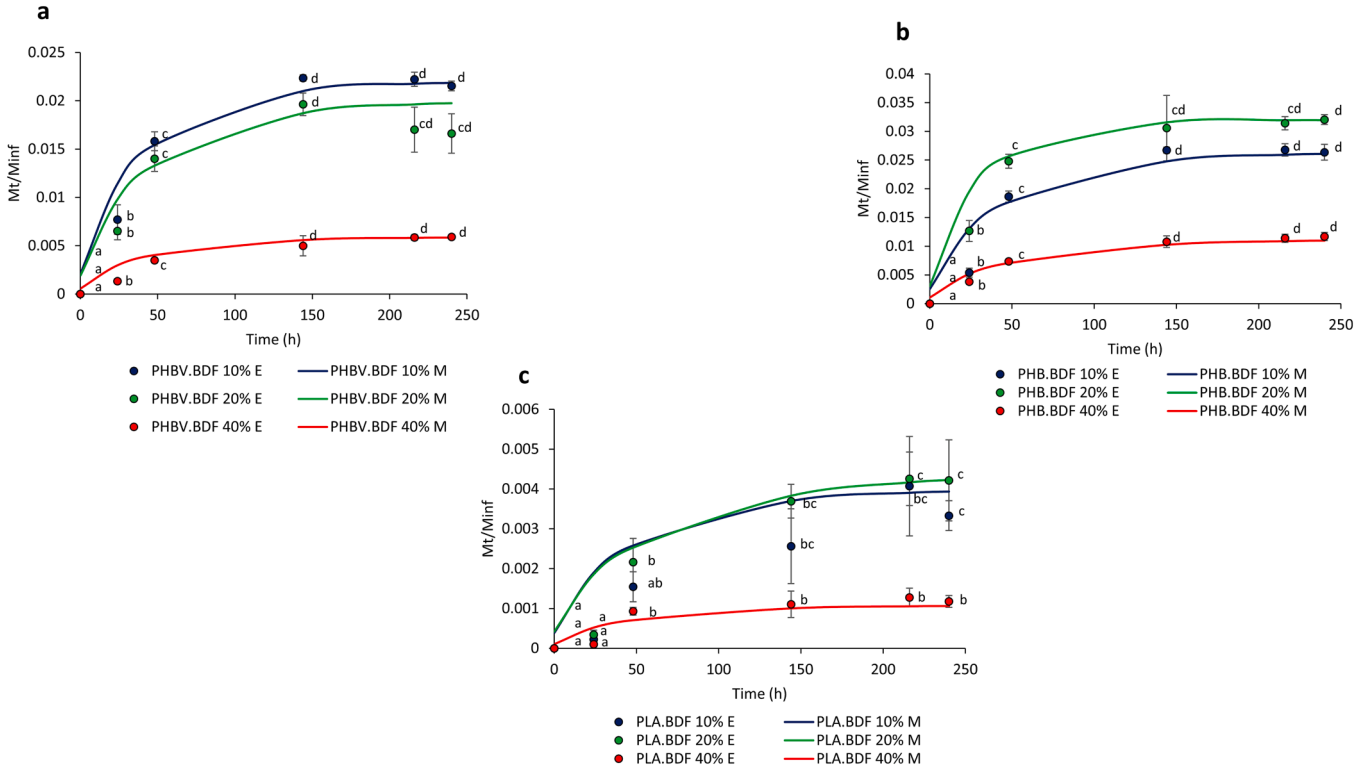

Fig. 1. Release kinetics and mathematical modelling of the BDF from different polymeric films. Whereas a) PHBV.BDF 10, 20 and 40 w%, b) PHB.BDF 10, 20, and 40 w% and c) PLA.BDF 10, 20, and 40 w%. (Different superscript letters (a-d) beside each point indicate significant ($p < 0.05$) differences among mean observations). Furthermore, dots represent experimental values and lines represent mathematical models used for fitting.

highest BDF content (40 w%). BDF is hydrophobic in nature thus a lower amount of BDF in the films means it has more affinity for hydrophilic food simulant (i.e., 10% ethanol), thus more release of BDF can be expected from films with lower BDF content. Furthermore, a higher percentage of BDF (40%) favoured the BDF-BDF interaction rather than the BDF-PHA interaction along with the formation of a crosslinking cluster of PHA-BDF-BDF-PHA structure that leaves the BDF trapped and then delays its release. The films with more BDF content are more elastomeric than the ones with a smaller amount which could be due to the $\pi - \pi$ stacking between the aromatic rings of the BDF molecules. Still, the released amounts were extremely low because of the nature of the simulant used.

In the case of PLA based systems, a release of < 0.5 w% of BDF could be due to several reasons a) polarity of the polymer/additive/simulant, b) PLA has better affinity for aromatic compounds as compared to PHAs due to its structure, c) as reported by Ordoñez et al. (2022a), during thermal processing, partial esterification of –OH end chain of PLA with ferulic acid could occur which can limit the compound release into the simulant, however this was not the case in our study, since no transesterification occurred as confirmed by NMR (Gallos et al., 2021), d) only $\geq$ 50% ethanol can cause relaxation of PLA matrix by penetrating polymer matrix and favouring the release of the bioactive, and e) molecular mobility and diffusion-controlled mass transfer could be limited due to glassy-state of the polymer in the absence of polymer relaxation at the release temperature, however at 40% w BDF content $\pi - \pi$ stacking between the aromatic rings of the BDF molecules was promoted which could restrict the release of BDF from the PLA films in amorphous phase (Ducruet, Domenek, Colomines, and Guinault, 2009; Ordoñez et al., 2022a).

On the other hand, PHB and PHBV displayed better release amounts (0.59–3.2%) since a) they are not in their glassy state and polymer relaxation up to some extent can be expected, b) both polymers and additives are hydrophobic in nature, and c) PHB showed a better release percentage than PHBV because PHB is more crystalline and brittle whereas PHBV contain more hydroxyvalerate monomers (Aramvash et al., 2016). Furthermore, the BDF started to hinder PHB crystallization at $\geq$ 20 w% content which could be correlated with better release of PHB as compared to PHBV (Longé et al., 2022).

On the other hand, no polymer swelling, relaxation, and degradation were observed for PLA-based films as opposed to what was reported in the literature due to the influence of ethanol-rich solutions on the polymer matrix. Thus it is safe to say that swelling-controlled model is not applicable in our scenario (Ordoñez et al., 2022b). Ordoñez et al. (2022a) similarly, reported $<$ 15% release of ferulic acid but in D1 food simulant since the phenolic OH-group in ferulic acid could form hydrogen bond through oxygen of ester group of the polymer, thus limiting the diffusion even in hydrophobic mediums.

3.3. Mathematical modelling

As mathematical models are useful in describing the release phenomena, they can be used to estimate the ability of an active package to restrict the oxidation kinetics. In this study, Fick's Second Law was solved numerically by using finite differences methodology for fitting of the experimental data and to describe the release of BDF from the film into the simulant. The experimental values of M_t/M_∞ as well as the fitted Fick's Model are shown in Fig. 1. The effective diffusivity for PHBV samples decreased linearly ($p < 0.05$) with increasing concentration of BDF in the polymer matrix because of increasing hydrophobicity and lower affinity for 10% ethanol which is relatively hydrophilic in nature. The D value is related to molecular mobility of the additive within polymer matrix and is influenced by several factors i.e., structural characteristics of the matrix, molecular weight of the additive, and solubility of the antioxidant compound (Benbettaïab, Assifaoui, Karbowiak, Debeaufort, and Chambin, 2016). Similarly, PHB samples with low BDF content (10–20 w%) displayed higher (2.2–2.5 times) D values as compared to the ones with highest BDF concentration. Similar trend was also observed for PLA films (Table 1). The higher retention can be correlated with the ability of BDF to establish charge-charge interactions with the polymer (Benbettaïab, Tanner, Cayot, Karbowiak, and Debeaufort, 2018). The PHB, PLA, and PHBV might interact with BDF through hydrogen bonding, dipole–dipole and dipole-charge. The mathematical models adequately described the release mechanism of BDF from different polymer systems indicating good linearity and fitting of experimental data with the model data with RMSE < 0.1 and $R^2 > 0.85$ (Khan et al., 2022). Our results are in accordance with the literature in which authors observed a fluctuating diffusion coefficient which was dependent on the polarity and concentration of the bioactive (Marvdashti, Yavarmanesh, and Koocheki, 2019; Ordoñez et al., 2022a). A very low partition coefficient (K) values were observed in our study for all the film samples ($<$0.03) which indicates that BDF has more affinity for the film samples as compared to the food simulant since BDF has two phenolic OH groups which can allow it to interact perfectly with hydrophobic polymer matrix i.e., PLA and PHAs. We observed a limited release ($<$3.5% of the content present in the film) of BDF from all packaging materials, in contrast to release of ferulic acid (for which ~8–15% have been reported) from PLA and PHBV systems due to differences in their structure, polarity of the simulant, and the temperature of release kinetics experiment (Hernández-García et al., 2022). A slow and limited release of the bioactive can restrict the active role of the additive in different food systems with high polarities. In our scenario, since no conventional plasticizer was added to the system apart from gaining advantage of the plasticizing properties of BDF (which don't seem enough to promote release), a conventional plasticizer i.e., glycerol/sorbitol can provoke the structural relaxation of polymer matrix and improve molecular mobility to promote diffusion (Longé et al., 2022; Ordoñez et al., 2022a).

3.4. FT-IR

The chemical finger printing of all the film samples to identify functional groups of interest and their interaction before and after release is presented is Figs. 2, 3 and 4. For PHBV samples, the main characteristic C—H stretching bands were observed around 1274 and 2974 cm^{-1} (Unalan, Colpankan, Albayrak, Gorgun, and Urkmez, 2016). The absorption band at 1274 cm^{-1} can also be assigned to C—O stretch (alkyl aryl ether group). C—H bending vibrations were observed at 1379 cm^{-1} (Unalan et al., 2016). CO and C-CH_3 stretching bands were detected around 1054 and 1044 cm^{-1}, respectively. The most intense PHBV absorption peak at ~1720 cm^{-1} can be associated with C═O stretching vibrations due to crystalline nature of the carbonyl group of PHBV. The presence of CH_2 groups can be validated by the peak around

Table 1
Melting and glass transition temperatures obtained from DSC curves for different polymeric films.

Samples	T_m (°C)	T_g (°C)
PHBV	155.5 (1.3)^{b}	−1.66 (0.04)^{c}
PHBV.BDF 10%	152.3 (0.8)^{b}	−11 (0.90)^{a}
PHBV.BDF 20%	147.6 (1.8)^{a}	−12.05 (0.42)^{a}
PHBV.BDF 40%	152.6 (1.5)^{b}	−8.29 (0.25)^{b}
PHB	165.2 (1.8)^{bc}	0.44 (0.08)^{c}
PHB.BDF 10%	168.3 (1.5)^{c}	1.16 (0.09)^{c}
PHB.BDF 20%	160.2 (2.2)^{b}	−2.99 (0.18)^{b}
PHB.BDF 40%	130.4 (4.7)^{a}	−11.27 (0.80)^{a}
PLA	148.3 (0.6)^{c}	56.2 (1.75)^{c}
PLA.BDF 10%	142.7 (2.1)^{b}	35.9 (1.24)^{b}
PLA.BDF 20%	140.9 (1.9)^{b}	32.09 (0.72)^{b}
PLA.BDF 40%	132.5 (1.9)^{a}	12.27 (2.92)^{a}

Different superscript letters (a–c) within each column indicate significant ($p < 0.05$) differences among mean observations for different polymeric formulations. Each value represents a mean of three replicates with the standard deviation in parentheses.

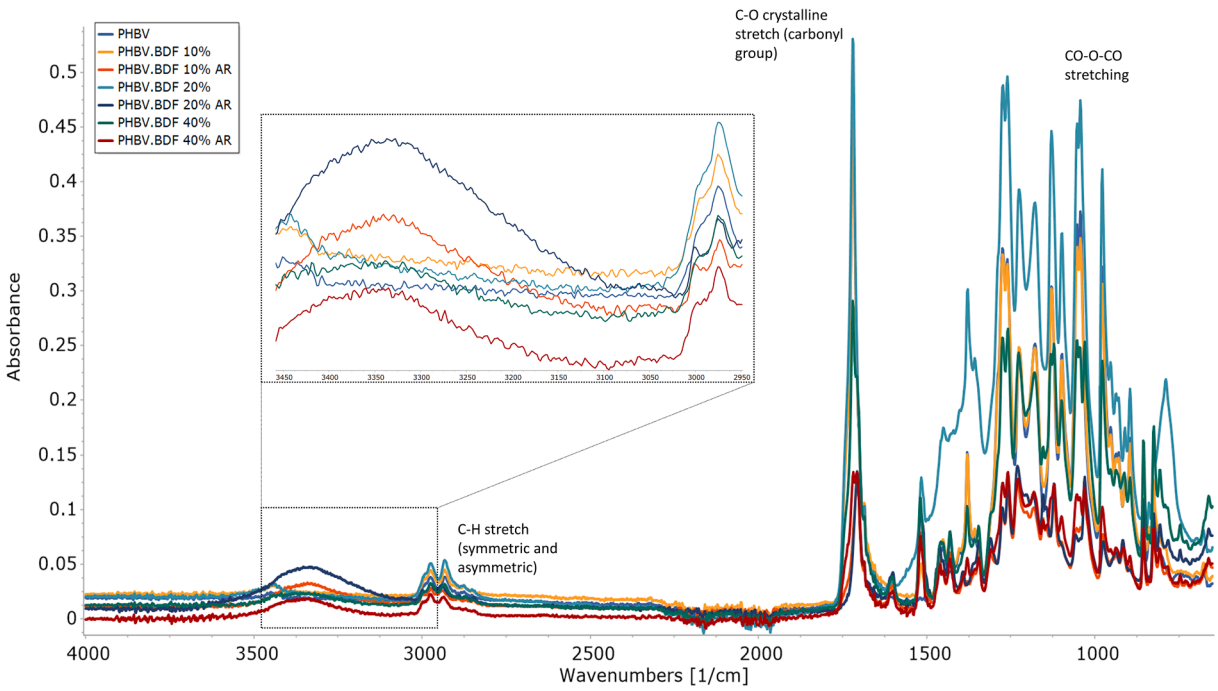

Fig. 2. FT-IR analysis of different PHBV films before and after release. Furthermore, AR means spectra recorded after release.

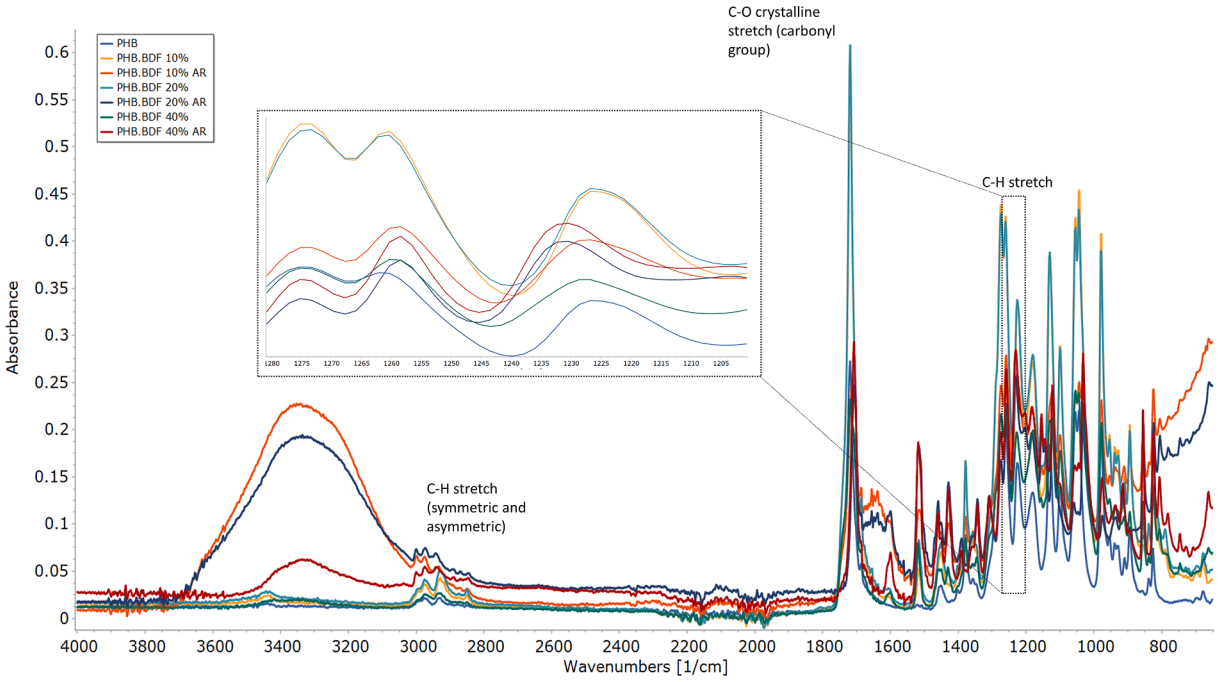

Fig. 3. FT-IR analysis of different PHB films before and after release. Furthermore, AR means spectra recorded after release.

2932 cm^{-1}. A broad peak between 3440 and 3450 cm^{-1} can be attributed to O—H stretching vibrations. Similar absorption spectra were observed for PHB films, for instance, C—O stretching at 1053 cm^{-1}, C—H bending at 1378 cm^{-1}, and C═O stretching at 1720 cm^{-1}. On the other hand, for PLA films, two characteristic peaks at 752 and 868 cm^{-1} were observed for crystalline and amorphous phases, respectively. The C═O stretching was observed as a large band at 1748 cm^{-1}. The most prominent peak (1080 cm^{-1}) was the rocking vibration of the helical backbone of CH_2 group. Other absorption peaks noticed were C—O stretching modes (~1180 cm^{-1}), CH_3 bending vibration (~1451 cm^{-1}), CH asymmetric deformation (1358 cm^{-1}), and CH stretching vibration (2995 cm^{-1}) (Siriprom, Sangwaranatee, Chantarasunthon, Teanchi, and Chamchoi, 2018). After incorporation of BDF into the blend, the C—O, O—H, and C—H stretching vibrations in PHBV and PHB films shifted to a lower wavenumber with reduced intensity with increasing concentration of BDF from 0 to 40 w% (from 1278 to 1228 cm^{-1}, ~3449 to ~3336 cm^{-1}, and ~2974 to ~2932 cm^{-1}, respectively), which could be due to weak interactions (dipole-dipole or hydrogen bonding) formed between polymer matrix and BDF. However, after the release kinetics, the aforementioned peaks shifted back again to their original

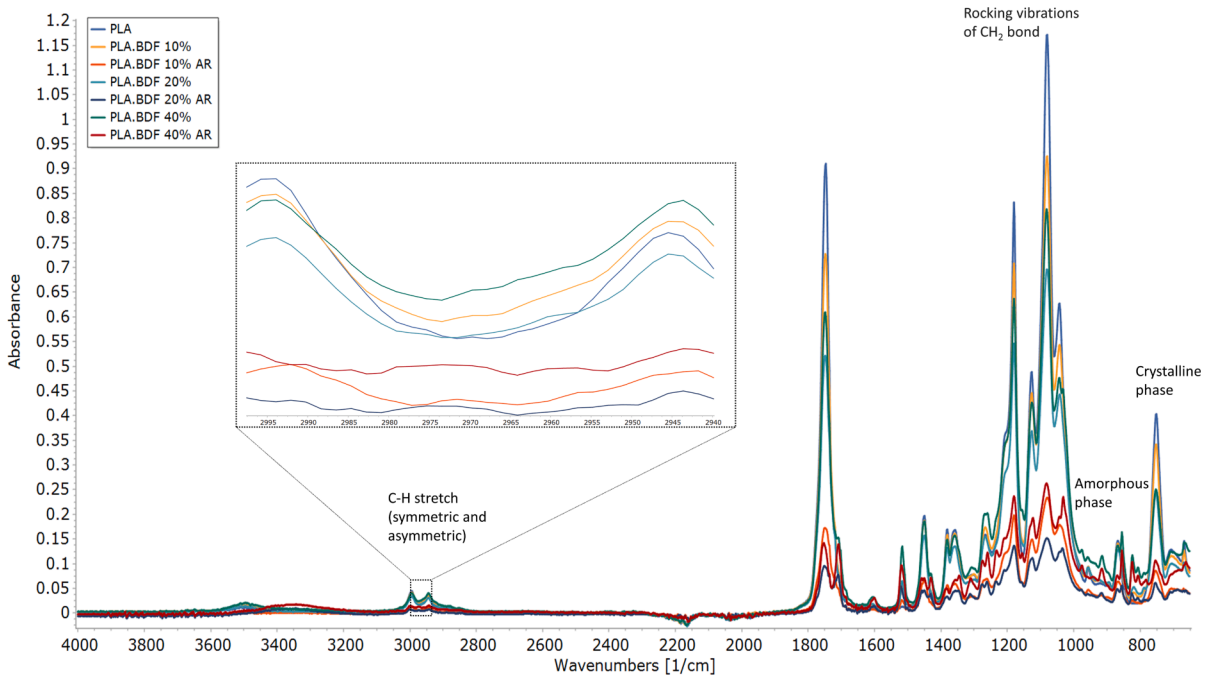

Fig. 4. FT-IR analysis of different PLA films before and after release. Furthermore, AR means spectra recorded after release.

wavenumber possibly due to the release of BDF from the polymer matrix causing the stretching of O—H and C—H groups upon cleavage by the food simulant. It was reported that stretching of C—H group could also be an indication of hydrogen bond formation between solvent molecules and polymer which can shift the frequency to higher wavenumbers (Kondo and Sawatari, 1996). The O—H stretching can also be an indication of intermolecular hydrogen bonding between OH group of the PHB/PHBV and carboxylic group of the BDF. Similarly, C—H stretch (2930–2980) and O—H bend were also reported be characteristic peaks for ferulic acid (Yerramathi et al., 2021). Disappearance of CH_3 asymmetric deformation after the addition of BDF in both PHB and PHBV films were observed, however, the peaks re-appeared after the release of BDF from the films, which indicates that BDF formed hydrogen bond with methoxy group of PHAs, however, these were easily cleaved by 10% ethanol leading to re-appearance of the peak (Kluth, Sung, and Maboudian, 1997). Contrarily, the spectra in the C—H stretching vibration shifted to lower wavenumber with increasing BDF content from 10 to 40% (from 2995 to 2943 cm^{-1}) only after its release from PLA films which is an indication of stronger interaction between PLA and BDF which led to significantly lower release than PHAs.

3.5. Antioxidant capacity

The antioxidant capacity of the active films containing BDF was assessed by using the method based on the scavenging of the DPPH·radical molecule. The DPPH-BDF reaction kinetics scheme is presented in the Fig. S1 as opposed to the reaction kinetics of ferulic acid with the DPPH (Goujot et al., 2019). It has been already established that ferulic acid is a slow antioxidant and require > 60 min of incubation with the DPPH· radical to finally reach plateau (Benbettaïeb et al., 2018; Goujot et al., 2019), since ferulic acid contains only one phenol (AHOH in reaction (1)) and can interact with DPPH· radical to form phenoxy radical which in-turn can interact with another DPPH· radical to form diferulic acids (reaction (4)) having two phenols (Goujot et al., 2019). However, these reactions are not required for the DPPH-BDF interaction since BDF has two phenols and can display faster reaction rate, thus reaction scheme can be modified and presented as in Fig. S1. Furthermore, oxidated BDF can be dismutated to regenerate a phenol, thus enhancing its antiradical property (Reano et al., 2015). The DPPH· interacted with BDF mainly by SET (single electron transfer) mechanism during which the antioxidant produces phenoxide anion that finally causes the reduction of the DPPH· radical. It has been reported that polar solvents (i.e., ethanol and methanol) can strongly bind with hydrogen atoms and reduce HAT (hydrogen atom transfer) mechanism and promote SET mechanism (Xie and Schaich, 2014). The antioxidant capacity results for control and active films displayed in Fig. 5 validate the above assumptions as there was no significant differences ($p > 0.05$) in the radical scavenging activity of BDF for both contact times since equilibrium was reached only after 30 min of incubation. The DPPH radical scavenging activity increased linearly with increasing concentration of the BDF in all the film samples. The PHBV and PHB samples containing 20–40 w% BDF displayed > 80% of DPPH inhibition. However, for PLA film samples containing 20–40 w% BDF, it was significantly lower (<75%) which could be due to stronger interaction of PLA with BDF due to its affinity for phenolic compounds. The residual purple colour only appeared in PLA samples with 10% w/w BDF content at the end of both analysis time (30 and 90 min). For all other samples, a change in colour of the solution from purple to yellow was observed since, at low BDF concentrations, there were no BDF-BDF interaction which could lead to a higher average percentage inhibition (but still non-significant) for 90 min contact time. However, this was not the case for higher concentrations (≥20 w%) (where BDF-BDF interactions or crosslinking cluster Polymer-BDF-BDF-Polymer) can hinder its full potential. The lower film antioxidant activity can be explained by interactions between the film matrix and active molecules in the film, limiting their release. PLA has stronger interactions with bioactives than PHAs so it can also affect the release kinetics and antioxidant properties even in highly hydrophobic media. All the control samples displayed extremely low antioxidant capacity (<5%) which is to be expected from PLA and PHAs since they do not have free residual amino groups, unlike protein/polysaccharide-based macromolecules whom free amino groups can be converted into ammonium groups by accepting hydrogen ions from DPPH solution. Thus, BDF has the potential to act as an antioxidant faster than ferulic acid in complex food systems, and to inhibit or restrict the nutritional losses caused by oxidation reactions.

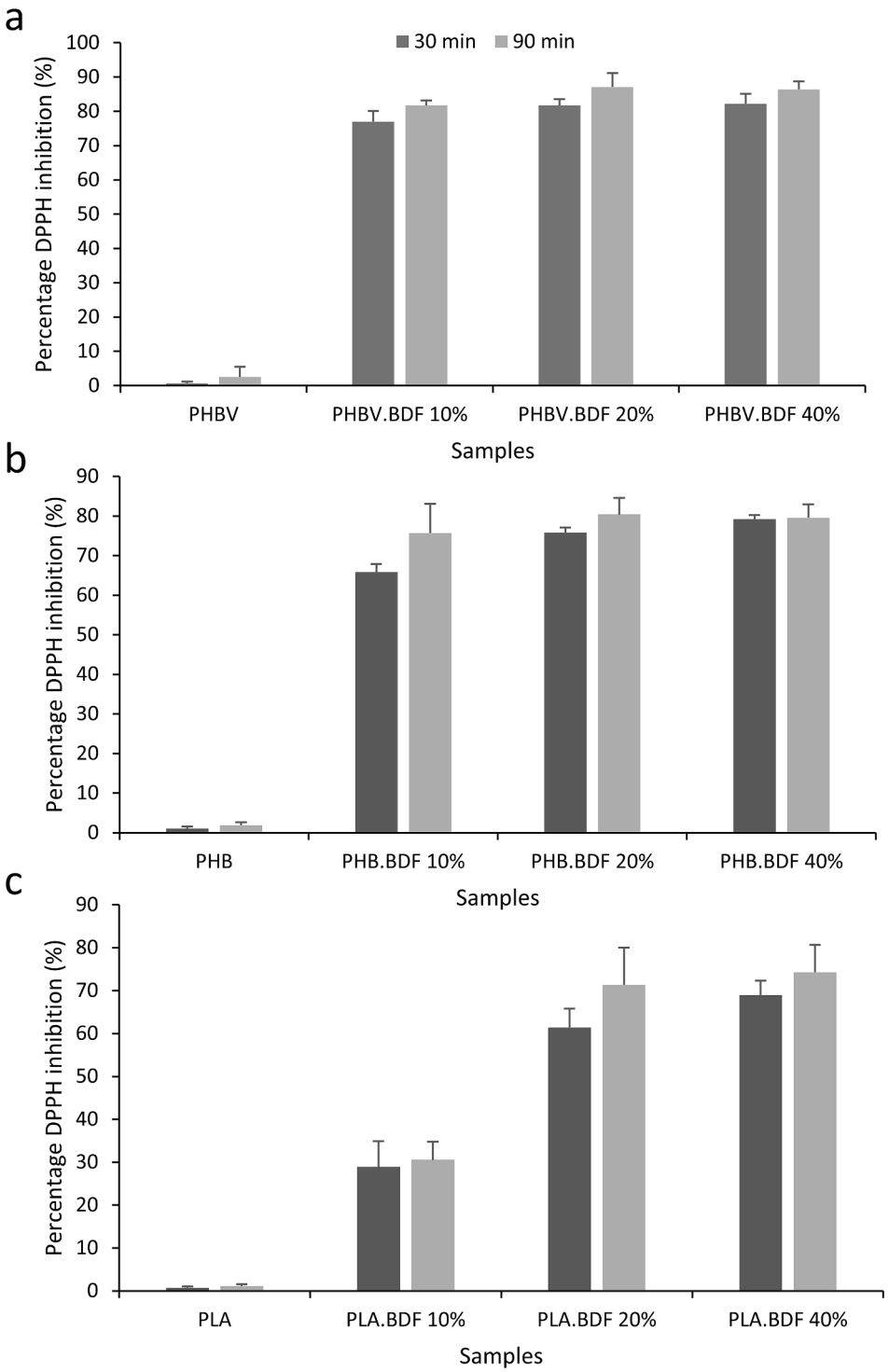

Fig. 5. Antioxidant capacity of the active films a) PHBV films, b) PHB films, and c) PLA films.

3.6. Thermal properties

The TGA curves for control and active films performed under a nitrogen atmosphere are shown in Fig. S2. The thermal stability of the polymer is commonly attributed to different parameters i.e., $T_{50\%}$ (temperature at 50% weight loss) and $T_{95\%}$ (temperature at 95% weight loss) (Table S2). The neat PHBV films displayed one-step thermal degradation between 245 and 280 °C. This thermal degradation was reported to proceed via the formation of an intermediate (six membered ring ester) having an alkenyl end and a carboxyl end group (Bakare, Bhan, and Raghavan, 2014). However, after incorporation of BDF into the PHBV films, the degradation proceeded in two steps, which indicates the formation of linkages between carboxyl group of the intermediate formed and hydroxyl group of the BDF. The highest weight loss (~45%) for PHBV films was observed between 266 and 277 °C, however, thermal stability significantly improved ($p < 0.05$) after incorporation of BDF into the blend. For example, similar weight loss for PHBV films containing 40% BDF was observed between 277 and 319 °C. The increased thermal stability of the films containing BDF could be due to presence of phenolic groups. A similar single-stage decomposition was observed for

neat PHB samples between ~250–280 °C due to β-elimination in ester moieties causing breakage of C—O and C═O bonds, which leads to the production of oligomers with terminal acid groups which in-turn get converted into crotonic acid and cause reduction in molecular weight (Etxabide et al., 2022). The maximum weight loss for PHB films (45%) was observed between (269–279 °C). However, the degradation occurred in two steps after the addition of BDF in the samples after the mass loss (between 50 and 95%) occurred at ~1.1–1.15 times higher temperatures as compared to control. As expected, once BDF was incorporated into the PHB matrix, $T5_{0\%}$ and $T_{95\%}$ were 1.1 to 1.15 times higher than those of the neat PHB samples. When considering PLA films, a two-stage thermal degradation appears to occur for all samples. During the first stage, all film samples were thermally stable till ~80 °C. The weight loss between (80–175 °C) can be attributed to bound moisture on the film surface. The second thermal degradation stage (280–385 °C) can be attributed to polymer back bone breakage due to thermal degradation and displayed maximum weight loss (Sucinda et al., 2021). The weight loss at the end of this stage decreased (from 98.07%, 95.29%, 93.32%, and 92.26%) with increase in the concentration of the BDF from 0, 10, 20, and 40 w%, respectively, which indicates strong interaction between BDF and PLA backbone that delayed thermal scission.

The DSC analysis was carried out to evaluate the thermal transitions of the films developed. The glass transition and melting temperatures (T_g and T_m) are shown in Table 1. The incorporation of BDF in the film samples brought changes in the thermal properties of the films. A significant decrease ($p < 0.05$) in melting and glass transition temperatures was observed for PHB samples after the incorporation of BDF into the blend which could be due to increased flexibility of the polymeric matrix (Carboué et al., 2022). The presence of BDF probably exerts two contrasting mechanisms to decrease T_g of the films, a) induction of the growth of large number of crystals which could have a nucleation effect on the polymer, and b) a decrease in crystal size because of imperfections (López-de-Dicastillo, Gómez-Estaca, Catalá, Gavara, and Hernández-Muñoz, 2012). Similarly, a decrease in T_m and T_g of the PLA samples (from 148.3 to 132.5 °C and 56.2 to 12.2 °C, respectively) was observed with increasing concentration of BDF from 0 to 40 w%. A semi-crystalline behaviour of PLA films was observed with a single T_g, which is an indication of full miscibility of both components in the amorphous phase. While a BDF of>20 w% inside polymer matrix led to crystallization due to a lack of interaction with PLA (Gallos et al., 2021). A reduction in T_m could be due to hydrogen interactions between phenolic hydroxyls and polyester carbonyls which can reduce crystal size and melting temperature (Hernández-García et al., 2022). Contrarily, incorporation of coumaric acid and protocatechuic acid (due to their structure) improved the T_g of the PLA and PHBV films due to improved interchain interactions (crosslinking) as compared to ferulic acid which can cause reduction of molecular mobility, thus inhibiting crystallization (Hernández-García et al., 2022). As expected, the T_g of the neat PHBV samples was extremely low (−1.66 °C). A further decrease in T_g of the PHBV films to −12.05 °C was observed after the incorporation of BDF up to 20 w%. However, an unexpected increase in T_g to −8.3 °C was recorded for PHBV films containing a higher amount of BDF (40 w%). This behavior can be attributed to the PHA-BDF-BDF-PHA interaction in the polymer film as BDF percentage increases beyond 20 w%, which might have restricted total crystallization of the polymer.

4. Conclusion

The total recovery of the active additive (BDF) in the casted films obtained from extruded blends was relatively high (86–93%) which indicates that this compound can be incorporated during the usual thermoplastic process in the packaging industry. Although no quantitative release of ferulic acid was detected in the Food Simulant A for the PLA-based films, we quantified the release of BDF from PLA matrix even though it was significantly lower (<0.5%) as compared to PHB and PHBV due to better affinity of PLA for phenolic acids. The slowest D values were observed for film samples containing 40 w% BDF content which could be correlated with their more hydrophobic nature as compared to lower concentrations. The addition of BDF into the polymer and its release also brought changes in the FT-IR spectra. We observed a comparatively faster DPPH reaction kinetics of BDF as compared to ferulic acid due to the presence of the biphenolic structure. The PHBV and PHB samples containing 20–40 w% BDF displayed > 80% of DPPH inhibition. However, for PLA film samples containing 20–40 w% BDF, it was significantly lower (<75%). The weight loss (between $T_{50\text{-}95}$%) for neat PHBV films containing 40% BDF (277–319 °C) was significantly higher than control (266–277 °C) due to formation of linkages between carboxyl group of the intermediate formed during thermal scission of PHBV and hydroxyl group of the BDF. The lowest release was observed for PLA films, however, they may still have great potential for packaging purposes. Further studies on release and antioxidant in food matrices are needed to test the ability of these films in real systems where polymer relaxation could facilitate compound migration to effectively limit oxidation kinetics to preserve nutritional quality of food products.

Declaration of Competing Interest

The authors declare that they have no known competing financial interests or personal relationships that could have appeared to influence the work reported in this paper.

Data availability

Data will be made available on request.

Acknowledgements

The PhD fellowship of Muhammad Rehan Khan is supported by MIUR and European Union's H2020 Project No. 817936. The 1st author also acknowledges Prof. Florent Allais for the support during his stay at URD-ABI AgroParisTech. The authors also thank Grand Reims, Département de la Marne and région Grand Est for their financial support.

Appendix A. Supplementary data

Supplementary data to this article can be found online at https://doi.org/10.1016/j.foodchem.2023.135395.

References

Aragón-Gutiérrez, A., Rosa, E., Gallur, M., López, D., Hernández-Muñoz, P., & Gavara, R. (2020). Melt-processed bioactive EVOH films incorporated with ferulic acid. *Polymers, 13*(1), 68. https://doi.org/10.3390/polym13010068

Aramvash, A., Hajizadeh-Turchi, S., Moazzeni-Zavareh, F., Gholami-Banadkuki, N., Malek-Sabet, N., & Akbari-Shahabi, Z. (2016). Effective enhancement of hydroxyvalerate content of PHBV in *Cupriavidus necator* and its characterization. *International Journal of Biological Macromolecules, 87*, 397–404. https://doi.org/10.1016/j.ijbiomac.2016.03.002

Bakare, R. A., Bhan, C., & Raghavan, D. (2014). Synthesis and characterization of collagen grafted poly (hydroxybutyrate–valerate)(PHBV) scaffold for loading of bovine serum albumin capped silver (Ag/BSA) nanoparticles in the potential use of tissue engineering application. *Biomacromolecules, 15*(1), 423–435. https://doi.org/10.1021/bm401686v

Benbettaïeb, N., Assifaoui, A., Karbowiak, T., Debeaufort, F., & Chambin, O. (2016). Controlled release of tyrosol and ferulic acid encapsulated in chitosan–gelatin films after electron beam irradiation. *Radiation Physics and Chemistry, 118*, 81–86. https://doi.org/10.1016/j.radphyschem.2015.01.035

Benbettaïeb, N., Tanner, C., Cayot, P., Karbowiak, T., & Debeaufort, F. (2018). Impact of functional properties and release kinetics on antioxidant activity of biopolymer active films and coatings. *Food Chemistry, 242*, 369–377. https://doi.org/10.1016/j.foodchem.2017.09.065

Carboué, Q., Fadlallah, S., Werghi, Y., Longé, L., Gallos, A., Allais, F., & Lopez, M. (2022). Impact of Bis-O-dihydroferuloyl-1, 4-butanediol Content on the Chemical, Enzymatic and Fungal Degradation Processes of Poly (3-hydroxybutyrate). *Polymers, 14*(8), 1564. https://doi.org/10.3390/polym14081564

Ducruet, V., Domenek, S., Colomines, G., & Guinault, A. (2009). Barrier properties of biodegradable polyesters towards aroma compounds. *National Research Council-Imcb University of Naples., 21*(2). https://www.itjfs.com/index.php/ijfs/issue/view/30/IJFS210-SLIM2008.

Etxabide, A., Kilmartin, P. A., Guerrero, P., de la Caba, K., Hooks, D. O., West, M., & Singh, T. (2022). Polyhydroxybutyrate (PHB) produced from red grape pomace: Effect of purification processes on structural, thermal and antioxidant properties. *International Journal of Biological Macromolecules, 217*, 449–456. https://doi.org/10.1016/j.ijbiomac.2022.07.072

Fiorese, M. L., Freitas, F., Pais, J., Ramos, A. M., de Aragão, G. M., & Reis, M. A. (2009). Recovery of polyhydroxybutyrate (PHB) from *Cupriavidus necator* biomass by solvent extraction with 1, 2-propylene carbonate. *Engineering in Life Sciences, 9*(6), 454–461. https://doi.org/10.1002/elsc.200900034

Foschi, E., & Bonoli, A. (2019). The commitment of packaging industry in the framework of the European strategy for plastics in a circular economy. *Administrative Sciences, 9*(1), 18. https://doi.org/10.3390/admsci9010018

Gallos, A., Crowet, J. M., Michely, L., Raghuwanshi, V. S., Mention, M. M., Langlois, V., … Allais, F. (2021). Blending ferulic acid derivatives and polylactic acid into biobased and transparent elastomeric materials with shape memory properties. *Biomacromolecules, 22*(4), 1568–1578. https://doi.org/10.1021/acs.biomac.1c00002

Goujot, D., Cuvelier, M. E., Soto, P., & Courtois, F. (2019). A stoichio-kinetic model for a DPPH•-ferulic acid reaction. *Talanta, 196*, 284–292. https://doi.org/10.1016/j.talanta.2018.12.056

Hernández-García, E., Vargas, M., & Chiralt, A. (2022). Effect of active phenolic acids on properties of PLA-PHBV blend films. *Food Packaging and Shelf Life, 33*, Article 100894. https://doi.org/10.1016/j.fpsl.2022.100894

Ibrahim, M. I., Alsafadi, D., Alamry, K. A., & Hussein, M. A. (2021). Properties and Applications of Poly (3-hydroxybutyrate-co-3-hydroxyvalerate) Biocomposites. *Journal of Polymers and the Environment, 29*(4), 1010–1030. https://doi.org/10.1007/s10924-020-01946-x

Kasmi, S., Gallos, A., Beaugrand, J., Paës, G., & Allais, F. (2019). Ferulic acid derivatives used as biobased powders for a convenient plasticization of polylactic acid in continuous hot-melt process. *European Polymer Journal, 110*, 293–300. https://doi.org/10.1016/j.eurpolymj.2018.11.036

Khan, M. R., Di Giuseppe, F. A., Torrieri, E., & Sadiq, M. B. (2021). Recent advances in biopolymeric antioxidant films and coatings for preservation of nutritional quality of minimally processed fruits and vegetables. *Food Packaging and Shelf Life, 30*, Article 100752. https://doi.org/10.1016/j.fpsl.2021.100752

Khan, M. R., Volpe, S., Salucci, E., Sadiq, M. B., & Torrieri, E. (2022). Active caseinate/guar gum films incorporated with gallic acid: Physicochemical properties and release kinetics. *Journal of Food Engineering, 335*, Article 111190. https://doi.org/10.1016/j.jfoodeng.2022.111190

Kluth, G. J., Sung, M. M., & Maboudian, R. (1997). Thermal behavior of alkylsiloxane self-assembled monolayers on the oxidized Si (100) surface. *Langmuir, 13*(14), 3775–3780. https://doi.org/10.1021/la970135r

Kondo, T., & Sawatari, C. (1996). A Fourier transform infra-red spectroscopic analysis of the character of hydrogen bonds in amorphous cellulose. *Polymer, 37*(3), 393–399. https://doi.org/10.1016/0032-3861(96)82908-9

Longé, L. F., Michely, L., Gallos, A., Rios De Anda, A., Vahabi, H., Renard, E., … Langlois, V. (2022). Improved Processability and Antioxidant Behavior of Poly (3-hydroxybutyrate) in Presence of Ferulic Acid-Based Additives. *Bioengineering, 9*(3), 100. https://doi.org/10.3390/bioengineering9030100

López-de-Dicastillo, C., Gómez-Estaca, J., Catalá, R., Gavara, R., & Hernández-Muñoz, P. (2012). Active antioxidant packaging films: Development and effect on lipid stability of brined sardines. *Food Chemistry, 131*(4), 1376–1384. https://doi.org/10.1016/j.foodchem.2011.10.002

Marvdashti, L. M., Yavarmanesh, M., & Koocheki, A. (2019). Controlled release of nisin from polyvinyl alcohol-*Alyssum homolocarpum* seed gum composite films: Nisin kinetics. *Food Bioscience, 28*, 133–139. https://doi.org/10.1016/j.fbio.2019.01.010

Niaz, T., & Imran, M. (2021). Diffusion kinetics of nisin from composite coatings reinforced with nano-rhamnosomes. *Journal of Food Engineering, 288*, Article 110143. https://doi.org/10.1016/j.jfoodeng.2020.110143

Ordoñez, R., Atarés, L., & Chiralt, A. (2022a). Effect of ferulic and cinnamic acids on the functional and antimicrobial properties in thermo-processed PLA films. *Food Packaging and Shelf Life, 33*, Article 100882. https://doi.org/10.1016/j.fpsl.2022.100882

Ordoñez, R., Atarés, L., & Chiralt, A. (2022b). Antilisterial action of PLA films with ferulic acid as affected by the method of incorporation. *Food Bioscience, 49*, Article 101865. https://doi.org/10.1016/j.fbio.2022.101865

Pion, F., Reano, A. F., Ducrot, P. H., & Allais, F. (2013). Chemo-enzymatic preparation of new bio-based bis-and trisphenols: New versatile building blocks for polymer chemistry. *RSC Advances, 3*(23), 8988–8997. https://doi.org/10.1039/C3RA41247D

Priyadarshi, R., Kim, S. M., & Rhim, J. W. (2021). Carboxymethyl cellulose-based multifunctional film combined with zinc oxide nanoparticles and grape seed extract for the preservation of high-fat meat products. *Sustainable Materials and Technologies, 29*, e00325.

Raghuwanshi, V. S., Gallos, A., Mendoza, D. J., Lin, M., Allais, F., & Garnier, G. (2022). Nanocrystallisation and self-assembly of biosourced ferulic acid derivative in polylactic acid elastomeric blends. *Journal of Colloid and Interface Science, 606*, 1842–1851. https://doi.org/10.1016/j.jcis.2021.08.123

Ramos, M., Jiménez, A., Peltzer, M., & Garrigós, M. C. (2014). Development of novel nano-biocomposite antioxidant films based on poly (lactic acid) and thymol for active packaging. *Food Chemistry, 162*, 149–155. https://doi.org/10.1016/j.foodchem.2014.04.026

Reano, A. F., Chérubin, J., Peru, A. M., Wang, Q., Clément, T., Domenek, S., & Allais, F. (2015). Structure–activity relationships and structural design optimization of a series of p-hydroxycinnamic acids-based bis-and trisphenols as novel sustainable antiradical/antioxidant additives. *ACS Sustainable Chemistry & Engineering, 3*(12), 3486–3496. https://doi.org/10.1021/acssuschemeng.5b01281

Requena, R., Vargas, M., & Chiralt, A. (2017). Release kinetics of carvacrol and eugenol from poly (hydroxybutyrate-co-hydroxyvalerate)(PHBV) films for food packaging applications. *European Polymer Journal, 92*, 185–193. https://doi.org/10.1016/j.eurpolymj.2017.05.008

Rojas, A., Velásquez, E., Patiño Vidal, C., Guarda, A., Galotto, M. J., & López de Dicastillo, C. (2021). Active PLA packaging films: Effect of processing and the addition of natural antimicrobials and antioxidants on physical properties, release kinetics, and compostability. *Antioxidants, 10*(12), 1976. https://doi.org/10.3390/antiox10121976

Santos, N. A., Cordeiro, A. M., Damasceno, S. S., Aguiar, R. T., Rosenhaim, R., Carvalho Filho, J. R., … Souza, A. G. (2012). Commercial antioxidants and thermal stability evaluations. *Fuel, 97*, 638–643. https://doi.org/10.1016/j.fuel.2012.01.074

Siriprom, W., Sangwaranatee, N., Chantarasunthon, K., Teanchai, K., & Chamchoi, N. (2018). Characterization and analyzation of the poly (L-lactic acid)(PLA) films. *Materials Today: Proceedings, 5*(7), 14803–14806. https://doi.org/10.1016/j.matpr.2018.04.009

Sucinda, E. F., Majid, M. A., Ridzuan, M. J. M., Cheng, E. M., Alshahrani, H. A., & Mamat, N. (2021). Development and characterisation of packaging film from Napier cellulose nanowhisker reinforced polylactic acid (PLA) bionanocomposites. *International Journal of Biological Macromolecules, 187*, 43–53. https://doi.org/10.1016/j.ijbiomac.2021.07.069

Tawakkal, I. S., Cran, M. J., Miltz, J., & Bigger, S. W. (2014). A review of poly (lactic acid)-based materials for antimicrobial packaging. *Journal of Food Science, 79*(8), R1477–R1490. https://doi.org/10.1111/1750-3841.12534

Unalan, I., Colpankan, O., Albayrak, A. Z., Gorgun, C., & Urkmez, A. S. (2016). Biocompatibility of plasma-treated poly (3-hydroxybutyrate-co-3-hydroxyvalerate) nanofiber mats modified by silk fibroin for bone tissue regeneration. *Materials Science and Engineering: C, 68*, 842–850. https://doi.org/10.1016/j.msec.2016.07.054

Woranuch, S., Yoksan, R., & Akashi, M. (2015). Ferulic acid-coupled chitosan: Thermal stability and utilization as an antioxidant for biodegradable active packaging film. *Carbohydrate Polymers, 115*, 744–751. https://doi.org/10.1016/j.carbpol.2014.06.074

Xie, J., & Schaich, K. M. (2014). Re-evaluation of the 2, 2-diphenyl-1-picrylhydrazyl free radical (DPPH) assay for antioxidant activity. *Journal of Agricultural and Food Chemistry, 62*(19), 4251–4260. https://doi.org/10.1021/jf500180u

Yerramathi, B. B., Kola, M., Muniraj, B. A., Aluru, R., Thirumanyam, M., & Zyryanov, G. V. (2021). Structural studies and bioactivity of sodium alginate edible films fabricated through ferulic acid crosslinking mechanism. *Journal of Food Engineering, 301*, Article 110566. https://doi.org/10.1016/j.jfoodeng.2021.110566